



Phase velocity of love waves as function of heterogeneity and void parameter

Sandip Kumar Das ¹, Anup Saha ^{*2}

¹Department of Mathematics (School of Advanced Sciences), VIT Chennai, Tamilnadu, India, skdkgpiit@gmail.com

²Department of Mathematics, Rampurhat College, Rampurhat-731224, India, sahaanup1989@gmail.com

Cite this study: Das, S. K., & Saha, A. (2024). Phase velocity of love waves as function of heterogeneity and void parameter. Turkish Journal of Engineering, 8 (4), 603-610.

<https://doi.org/10.31127/tuje.1442355>

Keywords

Love waves
Wave front
Whittaker's function
Void pores
Volume fraction

Abstract

The present study looks at the Love wave propagating through an elastic layer containing empty pores situated above a heterogeneous elastic semi-infinite space. We have constructed separate formulations of equations of motion for both media under congruous boundary conditions. The separation of variables approach is used to build the phase velocity frequency relation in compact form using the Whittaker function. The resulting closed-form dispersion equation matches the conventional Love wave equation when heterogeneity has been removed. The propagation of Love waves is strongly influenced by a porous layer of limited thickness across an elastic semi-infinite space. Three wave fronts are demonstrated to have the potential to propagate. The equilibrated inertia and the variation in the void volume fraction are related to two wave fronts that are connected to the characteristics of the void pores. Numerical treatments are applied and graphically illustrated to implement these effects associated to Love waves' phase velocity.

Research/Review Article

Received:
Revised:
Accepted:
Published:



1. Introduction

The way seismic waves travel around the Earth is significantly influenced by its layered structure. An abundance of data is supplied by Ewing et al. [1] regarding how seismic waves propagate. Love [2] developed a mathematical simulation of a specific kind of surface wave known as the Love wave. Many researchers, e.g. Achenbach [3], Pilant [4] etc. investigated how Love waves propagate in both homogeneous and heterogeneous space. Rayleigh waves are less susceptible to structural complexity than Love waves. Satô [5], [6], [7] and Noyer [8] created a model to show how Love waves move through a medium with various crustal thicknesses.

According to the current research, Love waves propagate under certain physical conditions that are

most likely found inside the Earth. Techniques for geophysical prospecting and surveying are necessary to examine how elastic waves propagate through porous media. A porous medium is defined as a solid or group of solid bodies that have enough space between them for a fluid to pass through or around them. Inherently porous and liquid-filled materials are common in the natural world. The mean distribution of the pores is uniform and their pore size is tiny. Numerous studies have stressed the importance of pore water in seismology. The dispersion of water and the readjusting of fluid pressure are what produce earthquakes. An elastic, porous, liquid-saturated medium has an established constitutive equation, according to Biot [9]. The Biot's hypothesis [10], [11] of fluid-saturated porous solids consolidated introduces numerous ideas on porous material's mechanical characteristics.

Nunziato and Cowin [12] postulated the existence of voids in a non-linear elastic material. Bulk density was stated as the result of multiplying the material matrix density by the volume fraction. The strain, the change in voids and void volume percentage are all regarded as independent kinematic variables in the linear theory of elastic material with voids. A substance that has sparsely spaced tiny spaces where there are none may be referred to as a porous substance. The field of geophysics & artificially produced porous substances have planned uses based on this theory. Applying Biot's theory to a porous media, Chattopadhyay et al. [13] discovered Love wave dispersion. According to Dey et al. [14], Love waves should propagate in an elastic layer containing empty pores.

The acceleration caused by gravity is essential to comprehending dynamic as well as static problems since Earth functions as a gravitational medium. As seismologists learn more about the Earth's structure, the gravitational impact of Love wave propagation is becoming more significant. Rayleigh wave's interaction with gravity in an incompressible half-space was demonstrated by Biot [15]. Love waves propagating in a transversely isotropic layer is significantly impacted by gravity as well as initial stresses, according to Dey et al. [16]. In a sand-filled, dry medium, Dey et al. [17] found that initial stress & gravity had an impact on torsional surface waves. Gupta et al. [18] compared the Rayleigh wave secular equations that are precise and approximate. The study conducted by Gupta et al. [19] aimed to examine the characteristics of wave propagation in carbon nanotubes.

Recently, Kumar et al. [20] showed that all of the material components of the model under discussion have a substantial effect on both the damped and phase velocity. A layered composite system's dynamic response to a load travelling on its upper rough surface with parabolic irregularity was examined by Gupta et al. [21]. Kumhar et al. [22] calculated the complex wave velocity of the SH-wave using the Fourier transformation method and Green's function. Gupta et al. [23] demonstrated the characteristics of the field variables by contrasting three distinct generalized thermoelastic models. Chowdhury et al. [24] looked at how irregularity and other influencing factors, such magnetic couplings and hydrostatic stresses, affected the propagation of waves. The electrical and mechanical displacements as well as the elements of electric potential have all been concurrently calculated by Maity et al. [25]. Kumar et al. [26] examined the Rayleigh wave's ability to travel through a piezoelectric-orthotropic substrate. Using a set of time-history natural ground motion records, Deringöl et al. [27] examined the seismic reactions of the fixed-base and base-isolated buildings. Using the criteria outlined in the aforementioned seismic codes, Ertuğrul et al. [28] examined yielding rigid retaining walls and anchored walls. Alam et al. [29] investigated the attenuation and dispersion characteristics of shear waves. The works done by Alam et al. [30], [31], Mario et al. [32], Singh et al. [33], [34] may also be cited.

In this problem, the feasibility of Love wave propagation over an inhomogeneous semi-infinite space in an elastic layer containing empty pores is studied. The

half space's inhomogeneity has been estimated to be $\mu = \mu_1(1 + az)$ and $\rho = \rho_1(1 + bz)$, where μ & ρ are the stiffness and mass density of the semi-infinite space respectively and the constants a and b have dimensions that are opposite to those of length. Bullen [35] discovered that as Earth's depth increases, so does its density. The layers' inherent non-uniformity may make this feasible. Brich [36] demonstrated in a different investigation that the stiffness of the Earth's strata varies at varying rates with depth. For this problem, Cowin and Nunziato's mechanics [37] of the elastic matrix with void pores are applied. We have established the velocity equation of Love waves in an elastic layer with void pores over a heterogeneous semi-infinite space. Three wave fronts are demonstrated to have the potential to propagate. The equilibrated inertia and the variation in the void volume fraction are related to two wave fronts that are connected to the characteristics of the void pores. The elasticity of the medium is linked to the other wave front.

2. Field equations and constitutive relationships

In the absence of body forces, Cowin and Nunziato [37] provide the following equations of motion for a homogeneous & isotropic porous elastic medium

$$\mu \nabla^2 \vec{u} + (\lambda + \mu) \nabla (\nabla \cdot \vec{u}) + \bar{\beta} \nabla \phi = \rho \frac{\partial^2 \vec{u}}{\partial t^2} \quad (1)$$

$$\bar{\alpha} \nabla^2 \phi - \xi \phi - \bar{\omega} \frac{\partial \phi}{\partial t} - \bar{\beta} \nabla \cdot \vec{u} = \rho \bar{k} \frac{\partial^2 \phi}{\partial t^2} \quad (2)$$

Where λ and μ are Lamé's moduli; $\bar{\alpha}, \bar{\beta}, \xi, \bar{\omega}$ & \bar{k} the functions of matrix volume fraction. ξ is a void parameter dependent on the inertial frame of reference; $u(x, t)$ stands for displacement vector; the difference in volume fraction from the reference volume fraction is represented by ϕ ; ρ is the medium's density and t is the time parameter.

Cowin and Nunziato [12] provide the relationship between stress and strain components as follows:

$$\tau_{ij} = \lambda \delta_{ij} e_{kk} + 2\mu e_{ij} + \bar{\beta} \phi \delta_{ij} (i, j = 1, 2, 3) \quad (3)$$

where δ_{ij} stands for the kronecker delta, τ_{ij} stress components and e_{ij} are strain components given by

$$e_{ij} = \frac{1}{2} \left(\frac{\partial u_i}{\partial u_j} + \frac{\partial u_j}{\partial u_i} \right).$$

2.1. Statement of the problem

Content We assume a heterogeneous semi-infinite space under an elastic layer of thickness H that has pores containing nothing. Both density and rigidity have been taken into consideration while discussing heterogeneity. In the lower space, the z -axis is oriented vertically downward. Along the path that the wave is moving in, the x -axis is selected to run along the layer. The layer-half space interface is where the origin is selected, as Fig. 1 illustrates.

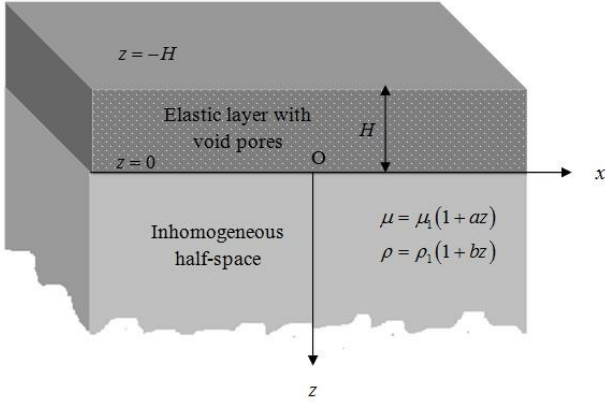


Figure 1. The Problem's Geometrical Shape.

Love waves have the displacement components $u = 0, w = 0$ & $v = v(x, z, t)$. The equations (1) and (2) that are not identically zero have the following form

$$\mu \left(\frac{\partial^2 v}{\partial x^2} + \frac{\partial^2 v}{\partial z^2} \right) + \bar{\beta} \left(\frac{\partial \phi}{\partial x} + \frac{\partial \phi}{\partial z} \right) = \rho \frac{\partial^2 v}{\partial t^2} \quad (4)$$

$$\bar{\alpha} \left(\frac{\partial^2 \phi}{\partial x^2} + \frac{\partial^2 \phi}{\partial z^2} \right) - \bar{\omega} \frac{\partial \phi}{\partial t} - \xi \phi = \rho \bar{k} \frac{\partial^2 \phi}{\partial t^2} \quad (5)$$

2.2. Analytical solutions for wave velocities

The solutions of equations (4) and (5) can be interpreted as follows for waves propagating at a velocity of c along x -axis pointing positively $v = \psi_1(z)e^{ik(x-ct)}$ and $\phi = \psi_2(z)e^{ik(x-ct)}$ where the equations satisfied by $\psi_1(z)$ & $\psi_2(z)$ are

$$\psi_1''(z) - N^2\psi_1(z) + B[ik\psi_2(z) + \psi_2'(z)] = 0 \quad (6)$$

And

$$\psi_2''(z) - M^2\psi_2(z) = 0 \quad (7)$$

Where $N = k(1 - (c^2/A^2))^{1/2}$, $B = \bar{\beta}/\mu$, $A = (\mu/\rho)^{1/2}$, $M = [(\bar{\alpha}k^2 - \rho\bar{k}k^2c^2 - i\bar{\omega}kct + \xi)/\bar{\alpha}]^{1/2}$, $\bar{\alpha}, \bar{k}, \xi$ representing constants specific to a certain substance. It is possible to interpret the value of M as follows while omitting the damping factor $\bar{\omega}$, which is negligible for sinusoidal waves

$$M = k \left[1 - \frac{c^2}{(\bar{\alpha}/\rho\bar{k})} + \frac{1}{k^2(\bar{\alpha}/\xi)} \right]^{1/2} \quad (8)$$

Solution of equation (7) with M as given in (8) may be taken as

$$\psi_2 = R_3e^{Mz} + R_4e^{-Mz} \quad (9)$$

Using (9), the solution of equation (6) becomes

$$\psi_1 = R_1e^{Nz} + R_2e^{-Nz} - \frac{B(ik + M)}{M^2 - N^2}e^{Mz}R_3 - \frac{B(ik - M)}{M^2 - N^2}e^{-Mz}R_4 \quad (10)$$

Hence the solution of equation (4) and equation (5) may be written as

$$v = \left[R_1e^{Nz} + R_2e^{-Nz} - \frac{B(ik + M)}{M^2 - N^2}e^{Mz}R_3 - \frac{B(ik - M)}{M^2 - N^2}e^{-Mz}R_4 \right] e^{ik(x-ct)} \quad (11)$$

$$\phi = [R_3e^{Mz} + R_4e^{-Mz}]e^{ik(x-ct)} \quad (12)$$

2.2.1. Solution for layer

Only The solution can be expressed as follows, with the upper layer's quantities indicated by the subscript 0

$$v_0 = \left[R_1e^{N_0z} + R_2e^{-N_0z} - \frac{B(ik + M_0)}{M_0^2 - N_0^2}e^{M_0z}R_3 - \frac{B(ik - M_0)}{M_0^2 - N_0^2}e^{-M_0z}R_4 \right] e^{ik(x-ct)} \quad (13)$$

$$\phi_0 = [R_3e^{M_0z} + R_4e^{-M_0z}]e^{ik(x-ct)} \quad (14)$$

Where $N_0 = k(1 - (c^2/A_0^2))^{1/2}$, $B_0 = \bar{\beta}_0/\mu_0$, $A_0 = (\mu_0/\rho_0)^{1/2}$ and $M_0 = k \left[1 - \frac{c^2}{(\bar{\alpha}_0/\rho_0\bar{k})} + \frac{1}{k^2(\bar{\alpha}_0/\xi_0)} \right]^{1/2}$.

2.2.2. Solution for half-space

The displacement caused by Love waves can be expressed in terms of an equation of motion as follows (Biot [15])

$$\frac{\partial s_{21}}{\partial x} + \frac{\partial s_{23}}{\partial z} = \frac{\partial^2}{\partial t^2}(\rho v) \quad (15)$$

Where s_{ij} represents the stress components in the semi-infinite space and ρ the density of the substance.

The inhomogeneity in the space has been assumed as

$$\mu = \mu_1(1 + az), \rho = \rho_1(1 + bz) \quad (16)$$

where $\mu = \mu_1, \rho = \rho_1$ at $z = 0$ and the variables a, b have inversely sized dimensions in relation to length.

Making use of the stress-strain relationships

$$s_{21} = 2\mu e_{xy}, s_{23} = 2\mu e_{yz} \quad (17)$$

and the relation (16), the equations of motion (15) becomes

$$\frac{\partial^2 v}{\partial x^2} + \frac{\partial^2 v}{\partial z^2} + \frac{a}{1 + az} \frac{\partial v}{\partial z} = \frac{\rho_1(1 + bz)}{\mu_1(1 + az)} \frac{\partial^2 v}{\partial t^2} \quad (18)$$

Let $v = \psi(z)e^{ik(x-ct)}$ be the solution of (18), then equation (18) reduces into

$$\frac{d^2\psi}{dz^2} + \frac{a}{(1+az)} \frac{d\psi}{dz} + \left[\frac{\rho_1(1+bz)}{\mu_1(1+az)} c^2 - 1 \right] k^2 \psi = 0 \quad (19)$$

Now by inserting $\psi = \frac{\phi(z)}{(1+az)^{1/2}}$ in equation (19) to get rid of $\frac{d\psi}{dz}$, we obtain

$$\frac{d^2\phi(z)}{dz^2} + \left[\frac{a^2}{4(1+az)^2} - k^2 \left\{ 1 - \frac{c^2(1+bz)}{c_1^2(1+az)} \right\} \right] \phi(z) = 0 \quad (20)$$

where $c_1 = \sqrt{\mu_1/\rho_1}$ and c the velocity of Love wave.

Substituting $\gamma_1 = \left[1 - \frac{c^2 b}{c_1^2 a} \right]^{1/2}$, $\eta_1 = \frac{2\gamma_1 k(1+az)}{a}$, $\omega = kc$ in equation (20), we get

$$\frac{d^2\phi(\eta_1)}{d\eta_1^2} + \left[\frac{R}{2\eta_1} + \frac{1}{4\eta_1^2} - \frac{1}{4} \right] \phi(\eta_1) = 0 \quad (21)$$

where $= \frac{\omega^2(a-b)}{c_1^2 a^2 \gamma_1 k}$.

The equation (21) has the solution $\phi(\eta_1) = R_5 W_{R/2,0}(\eta_1) + R_6 W_{-R/2,0}(-\eta_1)$, where $W_{R/2,0}(\eta_1)$ is the Whittaker's function [38]. Under the condition $\lim z \rightarrow \infty$ when $V(z) \rightarrow 0$ i.e. $\lim \eta_1 \rightarrow \infty$ when $\phi(\eta_1) \rightarrow 0$ the solution becomes

$$\phi(\eta_1) = R_5 W_{R/2,0}(\eta_1) \quad (22)$$

Thus, in the heterogeneous space, the displacement component is

$$v = \frac{R_5 W_{R/2,0}(\eta_1)}{(1+az)^{1/2}} e^{ik(x-ct)} \quad (23)$$

Equation (23) is reduced to when Whittaker's function is expanded to linear terms

$$v = v_1(\text{say}) = \frac{R_5}{(1+az)^{1/2}} e^{-\frac{\gamma_1 k(1+az)}{a}} \left\{ \frac{2\gamma_1 k(1+az)}{a} \right\}^{R/2} \left[1 - \frac{\left(\frac{R}{2} - \frac{1}{2}\right)^2 a}{2\gamma_1 k(1+az)} \right] e^{ik(x-ct)} \quad (24)$$

3. Boundary conditions

(i) References It is necessary for the stress component to remain continuous at $z = 0$, i.e.,

$$\mu_0 \frac{\partial v_0}{\partial z} = \mu_1 \frac{\partial v_1}{\partial z} \quad (25)$$

(iii) It is necessary for the displacement component to remain continuous at $z = 0$, i.e.,

$$(iv) \quad v_0 = v_1 \quad (25b)$$

$$(v) \quad \text{At, } z = -H \text{ the stress vanishes such that } \mu_0 \frac{\partial v_0}{\partial z} = 0 \quad (25c)$$

$$(vi) \quad \text{At, } z = 0 \text{ the boundary condition } \phi_0 \text{ is } \vec{n} \cdot \nabla \phi_0 = 0 \text{ i.e. } \frac{\partial \phi_0}{\partial z} = 0 \quad (25d)$$

where \vec{n} represents the unit vector perpendicular to the external boundary.

$$(vii) \quad \text{At, } z = -H \text{ the boundary condition } \phi_0 \text{ is } \vec{n} \cdot \nabla \phi_0 = 0 \quad (25d)$$

where \vec{n} represents the unit vector perpendicular to the external boundary.

Equations (13), (14) & (24) combined with aforementioned boundary conditions (25a)-(25e) result in

$$\mu_0 \left[R_1 N_0 - R_2 N_0 - \frac{B(ik + M_0)M_0}{M_0^2 - N_0^2} R_3 + \frac{B(ik - M_0)M_0}{M_0^2 - N_0^2} R_4 \right] - \mu_1 R_5 e^{-\frac{\gamma_1 k}{a}} \left\{ \frac{2\gamma_1 k}{a} \right\}^{R/2} P = 0 \quad (26)$$

Where

$$P = \left[\gamma_1 \left\{ 1 - \frac{\left(\frac{R}{2} - \frac{1}{2}\right)^2 a}{2\gamma_1 k} \right\} - \frac{a}{k} \left\{ \left(\frac{R}{2} - \frac{1}{2}\right) - \frac{\left(\frac{R}{2} - \frac{1}{2}\right)^2 a}{2\gamma_1 k} \left(\frac{R}{2} - \frac{3}{2}\right) \right\} \right] \quad (27)$$

Where

$$Q = \left\{ 1 - \frac{\left(\frac{R}{2} - \frac{1}{2}\right)^2 a}{2\gamma_1 k} \right\}$$

$$N_0 R_1 e^{-N_0 H} - N_0 R_2 e^{N_0 H} - \frac{B(ik + M_0)M_0}{M_0^2 - N_0^2} e^{-M_0 H} R_3 + \frac{B(ik - M_0)M_0}{M_0^2 - N_0^2} e^{M_0 H} R_4 = 0 \quad (28)$$

$$M_0 R_3 - M_0 R_4 = 0 \quad (29)$$

$$M_0 R_3 e^{-M_0 H} - M_0 R_4 e^{M_0 H} = 0 \quad (30)$$

Eliminating R_1, R_2, R_3, R_4 and R_5 from equations (26)-(30), we get

$$\begin{vmatrix} N_0 & -N_0 & -\frac{B(ik + M_0)M_0}{M_0^2 - N_0^2} & \frac{B(ik - M_0)M_0}{M_0^2 - N_0^2} & \frac{\mu_1}{\mu_0} e^{-\frac{\gamma_1 k}{a}} \left\{ \frac{2\gamma_1 k}{a} \right\}^{\frac{R}{2}} P \\ 1 & 1 & -\frac{B(ik + M_0)}{M_0^2 - N_0^2} & -\frac{B(ik - M_0)}{M_0^2 - N_0^2} & e^{-\frac{\gamma_1 k}{a}} \left\{ \frac{2\gamma_1 k}{a} \right\}^{\frac{R}{2}} Q \\ N_0 e^{-N_0 H} & -N_0 e^{N_0 H} & -\frac{B(ik + M_0)M_0 e^{-M_0 H}}{M_0^2 - N_0^2} & \frac{B(ik - M_0)M_0 e^{M_0 H}}{M_0^2 - N_0^2} & 0 \\ 0 & 0 & M_0 & -M_0 & 0 \\ 0 & 0 & M_0 e^{-M_0 H} & -M_0 e^{M_0 H} & 0 \end{vmatrix} = 0$$

The above determinant gives either,

$$M_0 = 0 \tag{31}$$

or,

$$\sinh(M_0 H) = 0 \tag{32}$$

or,

$$\begin{vmatrix} N_0 & -N_0 & \frac{\mu_1}{\mu_0} P \\ 1 & 1 & Q \\ N_0 e^{-N_0 H} & -N_0 e^{N_0 H} & 0 \end{vmatrix} = 0 \tag{33}$$

Equation (31) gives $k \left[1 - \frac{c^2}{(\bar{\alpha}_0/\rho_0 \bar{k}_0)} + \frac{1}{k^2(\bar{\alpha}_0/\xi_0)} \right]^{1/2} =$

i.e.

$$c = \left[1 + \frac{1}{(km_0)^2} \right]^{\frac{1}{2}} c_3 \tag{34}$$

This is the first-kind Love wave's velocity in the assumed model.

$$\tan \left[\left(\sqrt{\frac{c^2}{A_0^2} - 1} \right) kH \right] = \frac{\mu_1}{\mu_0} \frac{\left[\gamma_1 \left\{ 1 - \frac{\left(\frac{R-1}{2} \right)^2 \frac{a}{k}}{2\gamma_1} \right\} - \frac{a}{k} \left\{ \left(\frac{R-1}{2} \right) - \frac{\left(\frac{R-1}{2} \right)^2 \frac{a}{k}}{2\gamma_1} \left(\frac{R-3}{2} \right) \right\} \right]}{\left\{ 1 - \frac{\left(\frac{R-1}{2} \right)^2 \frac{a}{k}}{2\gamma_1} \right\} \sqrt{\frac{c^2}{A_0^2} - 1}} \tag{37}$$

where $R = \frac{\omega^2(a-b)}{c_1^2 a^2 \gamma_1 k}$ and $\gamma_1 = \left[1 - \frac{c^2 b}{c_1^2 a} \right]^{1/2}$

This is the Love wave dispersion equation in the assumed model and is dependent on the half-space's inhomogeneity parameter as well as the elastic parameters of the layer and half-space.

This study demonstrates that Love waves propagate in three wave fronts in elastic media with void pores: two of the wave fronts, given by equations (34) and (35) are dependent on the void pores' parameters, while the third wave front, given by equation (37) does not depend on any parameter related to the variation in the void volume pores.

Equation (32) gives $\sinh \left[1 - \frac{c^2}{(\bar{\alpha}_0/\rho_0 \bar{k})} + \frac{1}{k^2(\bar{\alpha}_0/\xi_0)} \right]^{1/2} kH = 0$
i.e.

$$c = \left[1 + \frac{1}{(km_0)^2} + \left(\frac{n\pi}{kH} \right)^2 \right]^{\frac{1}{2}} c_3 \tag{35}$$

where $m_0 = \left(\frac{\bar{\alpha}_0}{\xi_0} \right)^{\frac{1}{2}}$ stands for displacement parameter, $c_3 = \left(\frac{\bar{\alpha}_0}{\rho_0 \bar{k}} \right)$ is the shear wave velocity caused by the layer's changing void volume fraction, n is not a fractional number and k is the spatial frequency of a wave.

In the assumed model, equation (35) gives the velocity of the second form of Love wave.

Equation (33) yields

$$\tanh(NH) = \frac{\mu_1}{\mu_0} \frac{P}{NQ} \tag{36}$$

Substituting P and Q in equation (36) one gets

4. Particular case

When homogeneity occurs in the semi-infinite space, i.e. for $a \rightarrow 0, b \rightarrow 0$ the dispersion equation (37) becomes

$$\tan \left[kH \sqrt{\frac{c^2}{A_0^2} - 1} \right] = \frac{\mu_1}{\mu_0} \frac{\sqrt{1 - \frac{c^2}{c_1^2}}}{\sqrt{\frac{c^2}{A_0^2} - 1}} \tag{38}$$

It validates the solution to the topic under discussion and is well recognized classical outcome of the Love wave.

5. Numerical calculation & discussions

The following data have been collected in order to investigate the impact of inhomogeneity:

1) The rigidity and density in upper layer are considered as (Kumar and Vandana [39])

2) The rigidity & density in inhomogeneous lower space are considered as (Gubbins [40])

To highlight the significance of porosity and inhomogeneity on Love wave propagation, numerical calculations were conducted using equations (34), (35) and (37) with varying parameter values that corresponded to the aforementioned features.

The values of ν in numerical form have been computed from equation (34) and (35) for various values of ν . Also the values of ν in numerical form have been computed from equation (37) for various values of ν .

The dimensionless phase velocity c/c_s and the dimensionless wave number kH for various values of ν are displayed against each other in Fig. 2. The phase velocity has been found to decrease with increasing ν values.

In Fig. 3 and Fig. 4, the curves are plotted with c/c_s against kH for various values of $\nu = 0.5, 0.7, 0.9$ at $n=1, 2$ respectively. The phase velocity has been found to decrease as the value of ν grows.

Figure 5 shows the curves with phase velocity plotted against spatial frequency considering various values of the inhomogeneity parameter related to the medium's stiffness. For curves 1, 2, and 3, the value of ν has been considered to be 0.1, whereas the values of ν have been determined to be 0.3, 0.4, and 0.5, respectively. The velocity of the Love wave has been observed to rise with the value of ν in the half-space.

Figure 6 shows curves with phase velocity plotted against wave number considering various values of the inhomogeneity parameter related to medium density. The value of ν has been assumed as 0.4 whereas the value of ν is considered as 0.3, 0.4 and 0.5 for the curves 1, 2 and 3 respectively. It has been noted that the velocity of the Love wave decreases as the value of ν in the half-space grows.

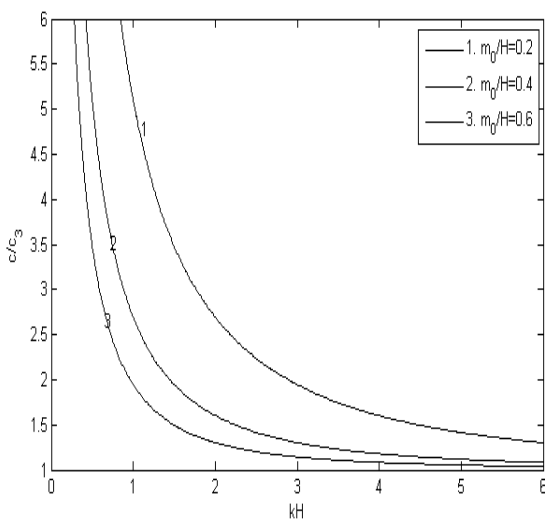


Figure 2. First kind Love wave dispersion curve with void pores for varying values of m_0/H .

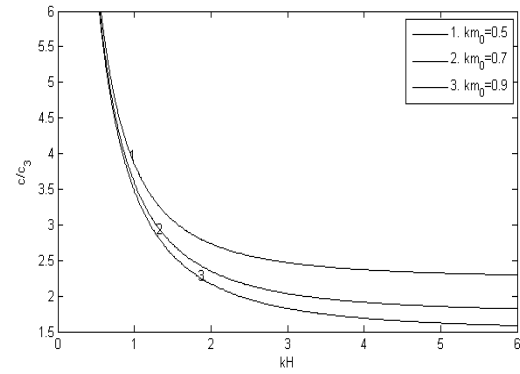


Figure 3. Second kind Love wave dispersion curve with void pores for varying values of km_0 at $n=1$.

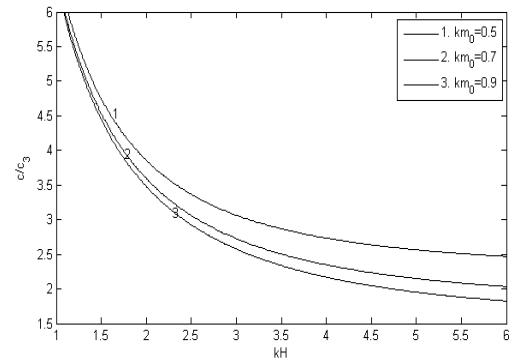


Figure 4. Second kind Love wave dispersion curve with void pores for various value of km_0 at $n=2$.

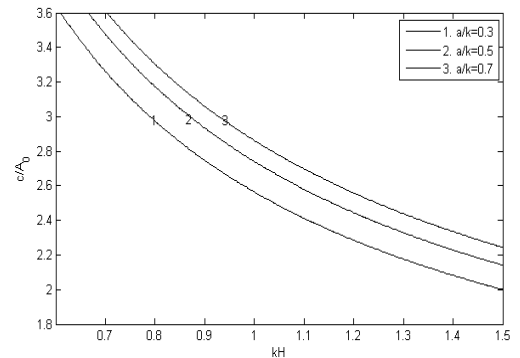


Figure 5. Influence of rigidity on Love wave propagation in the heterogeneous semi-infinite space for $b/k=0.1$.

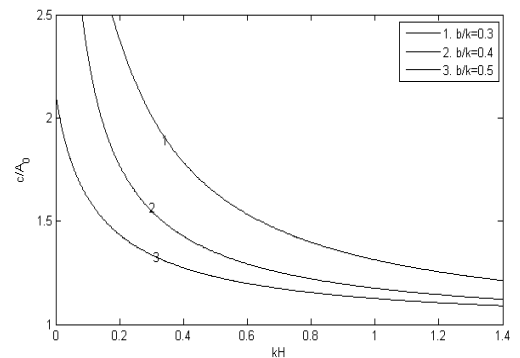


Figure 6. Impact of density on Love wave propagation in the heterogeneous semi-infinite space for $a/k=0.4$.

6. Discussion

Three Love wave fronts can persist in the medium concurrently, according to the study. The variation in the volume fraction of the pores determines two fronts. The third front is dependent on the medium's inhomogeneity characteristics and elastic constants. The following succinctly describes the conclusions drawn from the aforementioned analysis:

1. First and second kind Love waves' phase velocities decrease as the void parameter rises with dimensionless wave number.
2. While the inhomogeneity factor in rigidity has the opposite influence on the phase velocity, the inhomogeneity factor owing to linear variation in density in the inhomogeneous semi-infinite space decreases the phase velocity as it grows.
3. The dispersion equation (38) reduces to the generic Love wave equation in the case of a homogeneous layer over a homogeneous half-space.

Potential application in geophysical prospecting is the present thorough investigation of torsional surface waves in the assumed model. Knowing the origin and approximate damage from earthquakes is helpful. Additional applications for this research could be in-depth geologic structure mapping and oil drilling. Researchers in material science and designers of new materials may find usefulness in the findings reported in this study.

Acknowledgement

The authors are grateful to VIT Chennai and Rampurhat College for providing all necessary facilities for research.

Author contributions

Anup Saha designed, solved and validated the problem and Sandip Kumar Das sketched the curves, analyzed and interpreted the results and wrote the manuscript.

Conflicts of interest

On behalf of all authors, the corresponding author states that there is no conflict of interest.

References

1. Ewing, W. M., Jardetzky, W. S., & Press, F. (1957). *Elastic waves in layered media*. McGraw-Hill Book Co.
2. Love, A. E. H. (1944). *A treatise on the mathematical theory of elasticity*. Dover Publications.
3. Achenbach, J. D. (1973). *Wave propagation in elastic solids*. North-Holland Publishing Company.
4. Pilant, W. L. (1978). *Elastic waves in the earth*. Elsevier Scientific.
5. Satô, Y. (1952). Study on surface waves, V: Love waves propagated upon heterogeneous medium. *Bulletin of the Earthquake Research Institute*, 30, 1-12.
6. Satô, Y. (1952). Study on surface waves, VI: Generation of Love and other types of SH waves. *Bulletin of the Earthquake Research Institute*, 30, 101-120.
7. Satô, Y. (1952). Study on surface waves, VII: Travel time of Love waves. *Bulletin of the Earthquake Research Institute*, 30, 305-317.
8. Noyer, J. D. (1961). The effect of variations in layer thickness on Love waves. *Bulletin of the Seismological Society of America*, 51(2), 227-235.
9. Biot, M. A. (1955). Theory of elasticity and consolidation for a porous anisotropic solid. *Journal of Applied Physics*, 26, 182-185.
10. Biot, M. A. (1956). Theory of propagation of elastic waves in a fluid-saturated porous solid. I. Low frequency range. *Journal of the Acoustical Society of America*, 28(2), 168-178.
11. Biot, M. A. (1956). Theory of propagation of elastic waves in a fluid-saturated porous solid. II. Higher frequency range. *Journal of the Acoustical Society of America*, 28(2), 179-191.
12. Nunziato, J. W., & Cowin, S. C. (1979). A non-linear theory of elastic material with voids. *Archive for Rational Mechanics and Analysis*, 72, 175-201.
13. Chattopadhyay, A., Chakraborty, M., & Kushwaha, V. (1986). On the dispersion equation of Love waves in a porous layer. *Acta Mechanica*, 58, 125-136.
14. Dey, S., Gupta, S., & Gupta, A. K. (2004). Propagation of Love waves in an elastic layer with void pores. *Sādhanā*, 29, 355-363.
15. Biot, M. A. (1965). *Mechanics of incremental deformation*. John Wiley & Sons.
16. Dey, S., & Chakraborty, M. (1983). Influence of gravity and initial stresses on the Love waves in a transversely isotropic medium. *Geophysical Research Bulletin*, 21(4), 311-323.
17. Dey, S., Gupta, A. K., & Gupta, S. (2002). Effect of gravity and initial stress on torsional surface waves in dry sandy medium. *Journal of Engineering Mechanics*, 128, 1115-1118.
18. Gupta, S., Pramanik, S., & Smita. (2021). Exemplification in exact and approximate secular equation of surface wave along distinct interfaces with sliding contact. *Mechanics of Solids*, 56, 819-837.
19. Gupta, S., Pramanik, S., Smita, Das, S. K., & Saha, S. (2021). Dynamic analysis of wave propagation and buckling phenomena in carbon nanotubes (CNTs). *Wave Motion*, 104, 102730.
20. Kumar, D., Kundu, S., Kumhar, R., & Gupta, S. (2020). Vibrational analysis of Love waves in a viscoelastic composite multilayered structure. *Acta Mechanica*, 231, 4199-4215.
21. Gupta, S., Das, S., & Dutta, R. (2021). Nonlocal stress analysis of an irregular FGFP structure imperfectly bonded to fiber-reinforced substrate subjected to moving load. *Soil Dynamics and Earthquake Engineering*, 147, 106744.
22. Kumhar, R., Kundu, S., Pandit, D. K., & Gupta, S. (2020). Green's function and surface waves in a viscoelastic orthotropic FGM enforced by an impulsive point source. *Applied Mathematics and Computation*, 382, 125325.
23. Gupta, S., Das, S., Dutta, R., & Saha, S. (2021). Higher-order fractional and memory response in nonlocal

- double poro-magneto-thermoelastic medium with temperature-dependent properties excited by laser pulse. *Journal of Ocean Engineering and Science*. <https://doi.org/10.1016/j.joes.2022.04.013>
24. Chowdhury, S., Kundu, S., Alam, P., & Gupta, S. (2021). Dispersion of Stonely waves through the irregular common interface of two hydrostatic stressed MTI media. *Scientia Iranica*, 28(2), 837-846.
 25. Maity, M., Kundu, S., Kumhar, R., & Gupta, S. (2022). An electromechanical based model for Love type waves in anisotropic-porous-piezoelectric composite structure with interfacial imperfections. *Applied Mathematics and Computation*, 418, 126783.
 26. Kumar, D., & Kundu, S. (2023). Effect of initial stresses on the surface wave propagation in highly anisotropic piezoelectric composite media. *Waves in Random and Complex Media*. <https://doi.org/10.1080/17455030.2022.2164093>
 27. Deringöl, A. H., & Güneyisi, E. M. (2022). Enhancing the seismic performance of high-rise buildings with lead rubber bearing isolators. *Turkish Journal of Engineering*, 7(2), 99-107.
 28. Ertuğrul, O. L., & Zahin, B. B. (2022). A parametric study on the dynamic lateral earth forces on retaining walls according to European and Turkish building earthquake codes. *Turkish Journal of Engineering*, 7(3), 196-207.
 29. Alam, P., Jena, S., Badruddin, I. A., Khan, T. M. Y., & Kamangar, S. (2021). Attenuation and dispersion phenomena of shear waves in anelastic and elastic porous strips. *Engineering Computations*. <https://doi.org/10.1108/EC-07-2020-0381>
 30. Alam, P., Singh, K. S., Ali, R., Badruddin, I. A., Khan, T. M. Y., & Kamangar, S. (2021). Dispersion and attenuation of SH-waves in a temperature-dependent Voigt-type viscoelastic strip over an inhomogeneous half-space. *Journal of Applied Mathematics and Mechanics*. <https://doi.org/10.1002/zamm.202000223>
 31. Alam, P., Nahid, T., Alwan, B. A., & Saha, A. (2023). Rotating radial vibrations in human bones (femoral, mandibular and tibia) and crystals (Mg, Co, Cd, Zn and beryl) made cylindrical shell under magnetic field and hydrostatic stress. *Mechanics of Advanced Materials and Structures*, 30(13), 2684-2700.
 32. Mario, J. S., & Alam, P. (2023). A multi-layered model of Newtonian viscous liquid, fiber-reinforced and poro-elastic media over a self-weighted half-space to investigate the SH-wave interactions. *Mechanics of Advanced Materials and Structures*. <https://doi.org/10.1080/15376494.2023.2256537>
 33. Singh, M. K., & Alam, P. (2020). Surface wave analysis in orthotropic composite structure with irregular interfaces. *International Journal of Computational Mathematics*. <https://doi.org/10.1007/s40819-019-0745-5>
 34. Singh, M. K., Rahul, A. K., Saha, S., Paul, S., Tiwari, R., & Nandi, S. (2024). On generalized Rayleigh waves in a pre-stressed piezoelectric medium. *International Journal of Modern Physics C*. <https://doi.org/10.1142/S0129183124400060>
 35. Bullen, K. E. (1940). The problem of the Earth's density variation. *Bulletin of the Seismological Society of America*, 30(3), 235-250.
 36. Birch, F. (1952). Elasticity and constitution of the earth's interior. *Journal of Geophysical Research*, 57(2), 287-286.
 37. Cowin, S. C., & Nunziato, J. W. (1983). Linear theory of elastic materials with voids. *Journal of Elasticity*, 13, 125-147.
 38. Whittaker, E. T., & Watson, G. N. (1990). *A course in modern analysis*. Cambridge University Press.
 39. Kumar, R., & Vandana, G. (2013). Plane wave propagation in an anisotropic thermoelastic medium with fractional order derivative and void. *Journal of Thermal Stresses*, 1(1).
 40. Gubbins, D. (1990). *Seismology and plate tectonics*. Cambridge University Press.



© Author(s) 2024. This work is distributed under <https://creativecommons.org/licenses/by-sa/4.0/>